Journal of Archaeological Science 180 (2025) 106291

Contents lists available at ScienceDirect

Journal of Archaeological Science

journal homepage: www.elsevier.com/locate/jas

Reconstructing life history and ancestry from poorly preserved skeletal remains: A bioanthropological study of a Copper Age infant from Faenza (RA, Italy)

Owen Alexander Higgins [a,b,1,*], Francesco Fontani [a,c,1], Federico Lugli [d,e], Sara Silvestrini [a], Antonino Vazzana [a], Adriana Latorre [a], Massimo Sericola [f], Anna Cipriani [d,g], Gianluca Quarta [h], Lucio Calcagnile [h], Luca Bondioli [a,i], Alessia Nava [b], Elisabetta Cilli [a], Donata Luiselli [a], Stefano Benazzi [a]

[a] Department of Cultural Heritage, University of Bologna, Via degli Ariani 1, 48121, Ravenna, Italy
[b] Department of Odontostomatological and Maxillofacial Sciences, Sapienza University of Rome, Via Caserta 6, 00161, Rome, Italy
[c] Max Planck Harvard Research Center for the Archaeoscience of the Ancient Mediterranean, Max Planck Institute for Evolutionary Anthropology, Deutscher Platz 6, 04103, Leipzig, Germany
[d] Department of Chemical and Geological Sciences, University of Modena and Reggio Emilia, Via Giuseppe Campi 103, 41125, Modena, Italy
[e] Institut für Geowissenschaften, Goethe-Universität Frankfurt, Altenhöferallee 1, 60438, Frankfurt am Main, Germany
[f] Soprintendenza Archeologia, Belle Arti e Paesaggio per le province di Ravenna, Forlì-Cesena e Rimini, Via San Vitale, 17, 48121, Ravenna, Italy
[g] Lamont-Doherty Earth Observatory of Columbia University, 61 Route 9W, 10964, Palisades, NY, USA
[h] CEDAD (Centre of Applied Physics, Dating and Diagnostics), Department of Mathematics and Physics "Ennio De Giorgi", University of Salento, Via per Arnesano, 73100, Lecce, Italy
[i] Department of Cultural Heritage, University of Padova, Piazza Capitaniato 7, 35139, Padova, Italy

ARTICLE INFO

Keywords:
Preservation
Dental histology
aDNA
Palaeoproteomics
LA-ICPMS
Radiocarbon
Early life history

ABSTRACT

The poor preservation of archaeological skeletal remains, particularly those of infants, can result in partial representations of populations and significantly limit our understanding of the development and life of their infant segment. This study investigates the potential of combining dental histology, high spatial resolution biogeochemistry, radiocarbon dating, palaeoproteomic and ancient DNA (aDNA) analyses alongside traditional osteological methods to reconstruct the biological profile and life history of the heavily degraded skeletal remains of an infant from Faenza, Italy.

Severe skeletal degradation left only dental crowns and small osseous fragments, restricting traditional osteological analysis to an estimation of the age at death. Histological analysis of two dental specimens, a deciduous upper right first molar and a permanent lower right first molar, provided detailed insights into the infant's development, ultimately refining the age at death at approximately 17 months. Biogeochemical analysis using Laser Ablation-Inductively Coupled Plasma Mass Spectrometry (LA-ICPMS) revealed pronounced diagenetic alterations masking the original biogenic signal. Proteomic analysis of enamel peptides and genomic analysis of the osseous fragments identified the infant's sex as male. Genomic analysis, facilitated by a sufficient quantity of endogenous aDNA, enabled the reconstruction of the mitochondrial genome, providing valuable insights into the matrilineal ancestry of the individual and identifying an uncommon mtDNA haplogroup for the Eneolithic period in the Italian peninsula.

Despite the limited preservation of the skeletal elements, the combined application of advanced bioanthropological techniques demonstrated the substantial informative potential inherent in even a few preserved anatomical elements. This study underscores the critical value of multidisciplinary approaches in overcoming the challenges posed by highly degraded remains, revealing insights that would otherwise remain inaccessible.

* Corresponding author. Department of Cultural Heritage, University of Bologna, Via degli Ariani 1, 48121, Ravenna, Italy.
E-mail address: owen.higgins2@unibo.it (O.A. Higgins).
[1] These authors contributed equally.

https://doi.org/10.1016/j.jas.2025.106291
Received 18 November 2024; Received in revised form 15 May 2025; Accepted 8 June 2025
Available online 26 June 2025

1. Introduction

Human skeletal remains recovered from archaeological sites have the potential to provide invaluable insights into past populations and their lifeways. Understanding with the best precision possible the biological profile, life and genetic history of an individual, is crucial for reconstructing past populations and exploring various aspects of their lives. However, skeletal degradation frequently constrains the use of traditional osteological methods that rely upon good preservation of the skeletal elements. Various factors contribute to the deterioration of skeletal material over time, including environmental conditions, burial practices, and post-depositional processes, which can ultimately lead to extensive fragmentation and diagenetic alterations (Grupe, 2007; Wilson and Pollard, 2002).

The degradation of archaeological skeletal remains is a common issue encountered by researchers, with infant remains being particularly susceptible due to their fragile and developing skeletal structures. As a result, infant remains are regularly fragmentary, and often only isolated elements survive, making it challenging to reconstruct a biological profile, and comprehensively limiting our understanding of the development and life of this segment of the population (Bello et al., 2006; Manifold, 2012).

Among the most commonly surviving elements, teeth, auditory ossicles and the *pars petrosa* tend to survive better to post-depositional processes due to their compact shape and comparatively protected positions, as well as the high mineralization and density of the tissues comprising these elements. These characteristics confer a remarkable resistance to taphonomic and diagenetic alterations, while offering great insights into various aspects of human biology and population trajectories (Hillson, 2005; White and Folkens, 2005).

Teeth act as biological archives due to the rhythmic, incremental growth and general absence of remodelling of their tissues. These characteristics allow for the recording of significant information such as growth rates, physiological stresses, diet, environmental exposures, and mobility patterns during their development, all of which can be observed with high-temporal resolution (Dean, 1987, 2017; Higgins et al., 2024; Lugli et al., 2019a, 2022, 2019a; Mahoney, 2008, 2012, 2015; Müller et al., 2019a, 2024; Nava et al., 2020, 2024). Through incremental growth markers (e.g. daily cross-striations, as well as Retzius and Accentuated lines in dental enamel) it is possible to reconstruct a chronology specific to the tooth's development, providing insight into the foetal or postnatal stages depending on the tooth analysed (Higgins et al., 2024; Hodgkins et al., 2021; Mahoney, 2011, 2012, 2015; Nava et al., 2017a, 2017b, 2019). Moreover, if death occurred during dental development, age at death can be estimated with great accuracy (Dean et al., 1993b; Dirks, 1998; Higgins et al., 2024; Hodgkins et al., 2021; Nava et al., 2017b; Smith et al., 2011).

In addition, auditory ossicles and the *pars petrosa* of the temporal bone are commonly the preferred skeletal elements to sample for paleogenetic studies, as they have repeatedly proven to preserve elevated quantities of high-quality endogenous aDNA, often 100 times more than other bones, even in cases where other skeletal elements are severely degraded (Pinhasi et al., 2015; Sirak et al., 2020). However, sampling the petrous bone or ossicles is not always possible, especially when sample material is scarce or degraded. When *pars petrosa*, auditory ossicles and teeth are unavailable for aDNA investigation, other skeletal elements such as vertebrae, talus and phalanges have traditionally been considered viable alternatives (Parker et al., 2020). Even indeterminate bone fragments, though non-specific, can serve as sources for aDNA extraction in those cases when diagnostically informative bones are either absent or unsuitable for destructive analysis. Compact bone fragments may generally retain sufficient genetic material, offering an opportunity to retrieve significant genetic data, even when morphological analyses are limited or inconclusive.

In this study, we aim to explore the informative potential of the combination of dental histology, biogeochemistry, radiocarbon dating, palaeoproteomics and aDNA analyses in limit cases such as the extremely degraded skeletal remains of an infant discovered during an archaeological excavation in Faenza (Ravenna, Italy), for which only the dental crowns and fragments of undetermined skeletal remains were available. Our analysis enhanced the limited results obtainable from traditional osteological methods by combining them with histomorphometric examination and trace element analysis by Laser Ablation-Inductively Coupled Plasma Mass Spectrometry (LA-ICPMS) of two dental specimens, the palaeogenomic analysis on unidentified bone fragments, and palaeoproteomics on an enamel fragment. Despite the fragmentary state of the odontoskeletal elements, they retain substantial informative potential, allowing the investigation of various aspects of the infant's life history and ancestry that would otherwise remain inaccessible. Ultimately, this study intends to provide a guideline for high accuracy bioanthropological analysis capable of extracting in-depth information even from extremely poorly preserved remains. It contributes to recent osteobiographical objectives (Boutin, 2022; Hosek and Robb, 2019; Wrobel and Cucina, 2024), which emphasise the reconstruction of individual life histories and promote more nuanced interpretations of past human experiences beyond population-level generalisations.

2. Materials & methods

2.1. The site

The infant human remains were discovered during a commercial archaeological excavation preceding construction works in Via Romagnoli, near the city of Faenza (Ravenna, north-eastern Italy; Fig. 1a). The excavation area is characterized by multiple stratigraphic layers and pit features, with archaeological finds ranging in date from the Copper Age (also referred to as Eneolithic, approximately 4th - 3rd millennia BCE) to the Roman Age (3rd century BCE - 5th century CE).

The burial was found at a depth of −1.75 m, inside a large hole filled with layers of clay and ceramic remains, which was interpreted as the structure of a well that had likely already been abandoned at the time of the deposition (Fig. 1b).Although it is possible that wells and similar features were occasionally repurposed for burial, in this case the intentionality and cultural significance of the deposition remain uncertain in the absence of broader contextual information. The human remains consisted of a partial infant skeleton, in an extremely poor state of preservation, composed of the skull, part of the spine and part of the thorax. The bones were in anatomical connection and positioned with an east-west orientation, with the head facing south (Fig. 1c). Particular care was taken during recovery to preserve anatomical associations, with material separated by major anatomical portions when possible. However, due to the extremely poor preservation of the skeletal elements, most of the bones disintegrated during excavation and subsequent removal of sediment in the lab. Only the dental crowns were recovered intact. A few small osseous fragments, mostly composed of compact cortical bone, were collected, although their anatomical origin could not be determined.

At the same depth as the burial, which appeared as a plain deposition at the bottom of the well, there were fragments of ceramic vessels (Fig. 1b) in association with it. Among these, it is possible to identify three flask vases that have comparisons with Eneolithic contexts in central Italy and the Emilia area (Bagolini, 1981, 1984), as well as with archaeological sites in the Romagna area, such as the necropolis of Celletta dei Passeri in Forlì (Miari et al., 2017) and the cultual site of the Panighina, near the town of Bertinoro (FC, Italy) (Morico, 1996, 1997). These comparisons suggest an attribution of the infant's burial to the Italian Eneolithic (also referred to as the Copper Age), dated to approximately 3600-2300 BCE (Cocchi Genick, D., 2009).

2.2. Anthropological analysis

The skeletal remains were limited to identifiable dental crowns

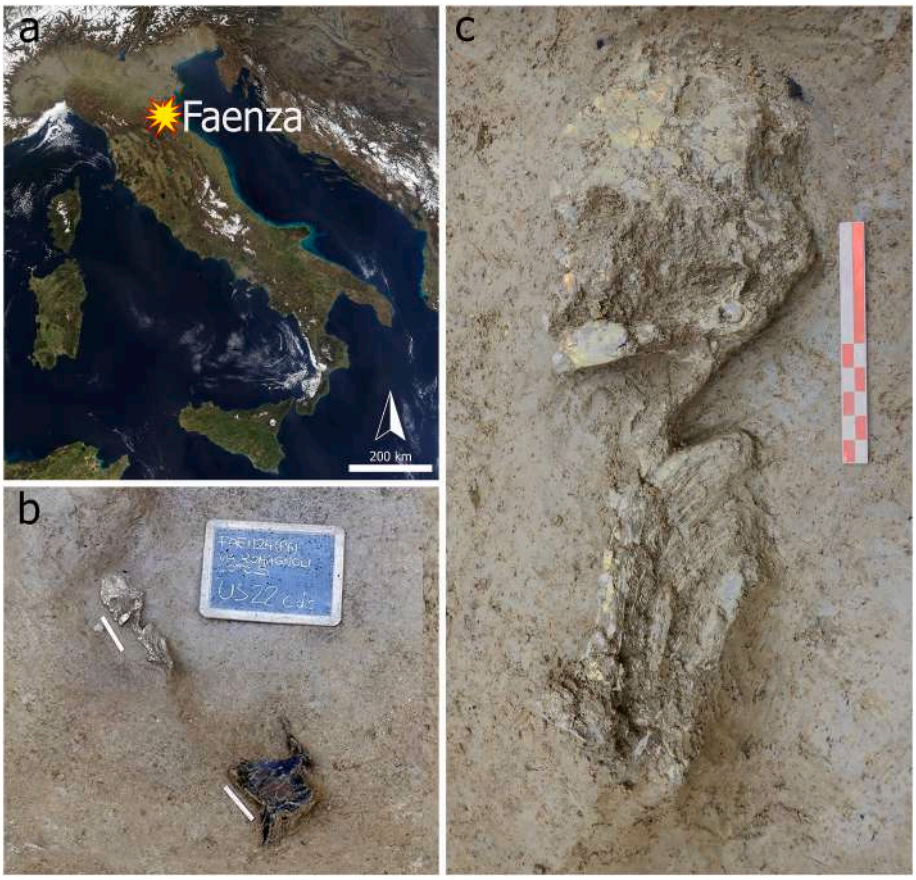

Fig. 1. Geographical location and archaeological context of the skeletal remains. a) Map of Italy (from NASA Visible Earth 1055 project – credits to Jacques Descloitres, MODIS Rapid Response Team, NASA/GSFC) showing the location of Faenza; b) Overview of the excavation unit, with associated artefacts visible; c) Close-up of the skeletal remains in situ. Photos by adArte Srl. Courtesy of the Ministry of Culture - Superintendence of Archaeology, Fine Arts, and Landscape for the provinces of Ravenna, Forlì-Cesena, and Rimini.

(Supplementary Fig. 1) and few unidentified bone fragments. As a result, the anthropological analysis focused on determining the developmental stage of the dental remains, utilising the criteria established by Moorrees et al. (1963a, 1963b). The age at death of the infant was subsequently estimated by correlating these developmental stages with the age ranges reported by AlQahtani et al. (2010).

2.3. Histological analysis

The deciduous upper right first molar (URdm^1; Fig. 2a) and the permanent lower right first molar (LRM$_1$; Fig. 2b) were selected for histological analysis due to their relatively good state of preservation and period of development based on known odontogenesis patterns for modern humans (AlQahtani et al., 2010; Hillson, 2005; Reid and Dean, 2006) to cover the broadest period of the infant's development, from the foetal stage to its premature death. Adapting Dean (2012) and Nava et al. (2020), both specimens were firstly embedded in epoxy resin (EpoThin™, Buehler) which was left to fully polymerise for 48 h at room temperature. The mesio-buccal cusp of both embedded teeth (the paracone for the URdm^1 and the protoconid for the LRM$_1$) was subsequently sectioned longitudinally along the bucco-lingual plane by using an Isomet™ Low Speed Saw (Buehler) mounted with a 0.3 mm thick diamond blade. The resulting exposed inner surfaces presenting the dentine horn were then gently grinded with P2500 abrasive paper and polished with 1 μm dye-free MetaDi™ Supreme Polycrystalline Suspension (Buehler) on a TriDent™ polishing cloth (Buehler). The polished surfaces were then rinsed with demineralised water and left to dry at room temperature. Once dry, the blocklets were pressed and glued on 1 mm thick glass slides with epoxy resin (EpoThin™, Buehler), which was left overnight to polymerise. Following, the blocklets were sectioned at ~300 μm of

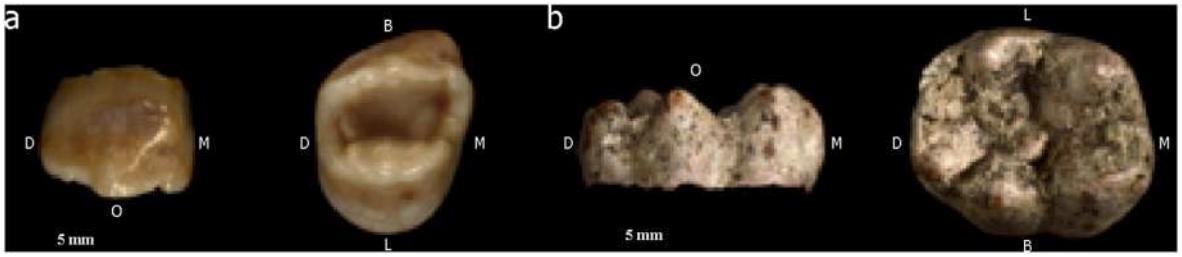

Fig. 2. Buccal and occlusal views of the deciduous upper right first molar (URdm1) and the permanent lower right first molar (LRM1) selected for histological analysis. (a) URdm1: buccal view (left) and occlusal view (right). (b) LRM1: buccal view (left) and occlusal view (right). Legend: B (Buccal), L (Lingual), M (Mesial), D (Distal), and O (Occlusal); Scale bar = 5 mm.

thickness with the Isomet™ Low Speed Saw (Buehler) mounting the 0.3 mm thick diamond blade. The resulting thin sections were finally grinded with P2500 abrasive paper to a thickness of ~150 μm, polished with 1 μm dye-free MetaDi™ Supreme Polycrystalline Suspension (Buehler) on a TriDent™ polishing cloth (Buehler) and rinsed with demineralised water.

At this point, biogeochemical analyses were performed on the thin section of the URdm[1]. Once the biogeochemical analyses were performed (see paragraph 2.4), the thin sections were furtherly grinded to approximately 100 μm and polished.

Mosaic micrographs of the sections were captured at various stages: prior to biogeochemical analyses, following these analyses to document the laser ablation tracks, and after the final polishing process. These micrographs were taken using transmitted polarized light at 100x magnification with an Axioscope7 microscope equipped with an Axiocam 305 color camera (Zeiss). The mosaic micrographs were automatically composed using the 'tile' tool within ZenCore v3.1 (Zeiss) software.

Individual-specific odontochronology was reconstructed for each crown following Birch and Dean (2014). Utilising Adobe Photoshop (Adobe Inc.), a segment following the local prism directionality was traced from the dentine tip to a visible Retzius line within 100 μm from the EDJ. The Retzius line (representing a synchronous moment in time) was then followed back to the EDJ, and the process was repeated along the EDJ to the end of the crown.

In correspondence of each selected prism segment, a minimum of six series of consecutive cross-striations (indicative of the daily secretion of enamel matrix; Antoine et al., 2009) were measured, and the length of each series was divided by the corresponding count of cross-striations. The computed average from this calculation was employed to estimate the local mean daily secretion rate (DSR) of enamel.

The duration of formation for each prism segment was estimated by dividing its length by the local mean DSR. The total crown formation time (CFT) was derived from the summation of the formation times of all selected prisms. Crown initiation (Ci) and completion (CrC) were calibrated using the position of the neonatal line (NNL; marking the moment of birth; Sabel et al., 2008), as observed in the URdm[1]. In the LRM_1, where a clear NNL was not evident, crown initiation was posited to align with birth, in accordance with established odontogenesis timelines (AlQahtani et al., 2010; Hillson, 1996; Reid et al., 1998).

Enamel extension rates (EERs) for each tooth were calculated by dividing the length of the EDJ between two selected prism segments by the number of days represented by the corresponding prism segment. The average EER for the crown was estimated by dividing the total length of EDJ by the estimated CFT.

Crown formation parameters were estimated on the paracone for the URdm[1] and on the protoconid for the LRM_1 since the section planes were centred based on the dentine horn of these cusps, allowing crown formation to be observed from Ci.

All measurements were conducted using ImageJ 1.54b software (Schindelin et al., 2012).

2.4. Trace element analysis

Spatially-resolved elemental analyses were conducted on the same thin sections used for the histological investigation of the URdm[1]. The analyses were carried out at the "Centro Interdipartimentale Grandi Strumenti" of the University of Modena and Reggio Emilia using a NewWave UP 231 nm Nd:YAG laser ablation system coupled to a Thermo Fisher Scientific iCAP-TQ ICPMS, closely following analytical protocols described by (Müller et al., 2019a). Ablation tracks of ~20 μm of width were performed in continuous profiling mode, consistently following the EDJ from dentine horn to cervix (maintaining a proximity within 100 μm) on both buccal and lingual aspect, and along selected prisms from the EDJ to outer enamel on the buccal aspect. The analysis focused on key trace elements commonly used to assess both biogenic signals and diagenetic alteration. Uranium (U) and manganese (Mn) were considered primary diagenetic proxies due to their characteristic post-depositional incorporation into dental tissues (Grimstead et al., 2018; Grün et al., 2008; Reynard and Balter, 2014). Lead (Pb), while also susceptible to diagenetic contamination, was included for its potential to reflect in vivo environmental exposure when preserved in its biogenic form (Budd et al., 2004; Kamenov et al., 2018; Shepherd et al., 2012; Smith et al., 2018). Strontium-to-calcium (Sr/Ca) and barium-to-calcium (Ba/Ca) ratios were analysed as dietary proxies, particularly for the investigation of nursing and weaning patterns, although these signals may also be affected by diagenetic processes (Austin et al., 2013; Higgins et al., 2024; Müller et al., 2019b, 2024; Nava et al., 2020, 2024; Smith et al., 2018). The primary aim of the trace element analysis was therefore twofold: to assess the extent of diagenetic overprinting and to evaluate the potential for reconstructing dietary practices and environmental exposure from the enamel record.

As mentioned above, a mosaic micrograph of the thin section displaying the tracks created by the ablation was taken at 100x magnification using episcopic polarised light with an Axioscope 7 microscope mounting a 208 color camera (Zeiss). Several micrographs were automatically taken and assembled into a composite image using the 'tile' tool on the ZenCore v3.1 software (Zeiss). Subsequently, the micrograph was imported in Adobe Photoshop (Adobe Inc.) and superimposed onto the micrograph used for the histomorphometric analysis and onto the chronological framework. This superimposition allowed the temporal attribution of multiple points along the ablation tracks. The distance of each temporally-attributed point along each ablation track was recorded using ImageJ 1.54b software (Schindelin et al., 2012). The translation of this spatial information into enamel (secretion) chronologies along the tracks, as well as the smoothing of the elemental profiles, were carried out using R software environment for statistical computing (v 4.2.3) (R Core Team, 2023) and a local polynomial regression fitting (Cleveland et al., 1992), following (Higgins et al., 2025).

2.5. Genomic analysis

All the laboratorial genetic analyses were performed at the ancient DNA facilities of the University of Bologna. Here, working professionals strictly adhered to the standard criteria for the handling and management of ancient DNA analysis in order to avoid contamination of the samples that could invalidate the final results (Cilli, 2024). A highly fragmented osseous element, measuring less than 1 cm and composed primarily of compact cortical bone, was isolated for ancient DNA extraction and transferred to the sterilised clean room of the ancient DNA laboratory dedicated for sampling of skeletal material. Its selection was based on the relative compactness and macroscopic preservation of the fragment, despite the inability to determine its anatomical origin. The bone was cleaned with a brush soaked in 4 % HCl, rinsed in 80 % EtOH and then sterilised under UV-light for 20 min. Due to the very fragile nature of the remains, sampling of the bone was performed by powdering the fragments on a sterilised mortar for DNA extraction. DNA isolation was later performed from 70 mg of bone powder in a separate room, following extraction protocols described in Fontani et al. (2023) – modified from Dabney et al. (2013) – and blank controls were processed along with the sample during each step of the laboratorial analysis. Briefly, the sample was digested for 15 h at 37 °C in a solution composed of 2700 μL of 0.5 M EDTA (pH 8), 37.5 μL of 20 mg/ml of proteinase K and water. We added PB binding buffer (Qiagen, Hilden, Germany) to the supernatant and transferred it into silica columns (Roche-High Pure Viral Nucleic Acid Large Volume Kit, Roche, Basel, Switzerland). Two washing steps with PE buffer (Qiagen) were performed before eluting the DNA in 40 μL of EB buffer (Qiagen). The presence of genetic material was confirmed by measuring the raw extracts on a QuBit fluorometer, then single-stranded genomic libraries were built for the extract according to Kapp et al. (2021), without enzymatic damage repair steps. A qPCR quantification was performed prior to indexing to identify the

cycle threshold. Then the library was indexed using a unique combination of two indexes. After purification, the indexed library was pooled in equimolar amounts with other samples, quantified on Agilent 2100 Bioanalyzer, and screened for endogenous DNA on HiSeqX Ten 2x75bp lane. An aliquot of 20 μL indexed library was separately enriched for human mitochondrial DNA (mtDNA) using a bait-capture method based on long-range PCR products (Maricic et al., 2010). The captured libraries were quantified using Agilent 2100 Bioanalyzer and sequenced on an Illumina MiSeq platform. The sequencing was run as paired-end with 75 × 2 + 8 + 8 cycles.

We used nf-core/eager v2.4.7 (Fellows Yates et al., 2021) for downstream analysis. Raw data were preliminary checked on fastqc, and the demultiplexed fastq sequences from shotgun sequencing were mapped to the GRCh37 nuclear reference genome using 'bwa aln' as mapper tool, disabling the seed option and setting a mapping quality threshold >30. Duplicates were removed using 'markduplicates', and general statistics were obtained through MultiQC (Ewels et al., 2016) and samtools (Danecek et al., 2021). We used DamageProfiler (Neukamm et al., 2021) for calculating and observing frequency ratio of deamination patterns along the 5′ ends of the sequences. For mtDNA enriched data, we merged reads from shotgun and capture sequencing and aligned them to an elongated version of the rCRS generated using Circular Mapper and 'bwa aln', setting general parameters for mapping as above. After evaluating the presence of deamination patterns, modern human contamination was estimated at mitochondrial level using Schmutzi (Renaud et al., 2015). Schmutzi was also employed to reconstruct both the endogenous and the potentially contaminated mitogenomes. We used Haplogrep3 (https://haplogrep.i-med.ac.at/) to infer the mitochondrial haplogroup of the individual, and cross compared the results by manually investigating the aligned sequences on IGV (Robinson et al., 2011). Biological sex of the individual was finally estimated by computing the ratio of reads aligning to the X-chromosome as a portion of the total sequences mapping to the autosomes, using the R script provided in Mittnik et al. (2016).

2.6. Proteomic analysis

Paleoproteomic analysis was performed on a loose fragment of enamel that weighed approximately 20 mg. Initial sample collection and preliminary processing were undertaken at the BONES Lab's proteomic facility within the Department of Cultural Heritage at the University of Bologna. Thorough removal of any adhering dentine residues was ensured through the use of a dentist drill. The sample was subsequently rinsed with MilliQ water in an ultrasonic bath and briefly subjected to a 5 % HCl leaching process. To extract enamel peptides, the enamel fragment was immersed in 200 μl of 5 % HCl for 1 h. The resulting supernatant was then purified using C_{18} in-house stage tips. Resin-bound peptides were eluted using 50 μL of a solution comprising 60 % acetonitrile in 0.1 % formic acid.

The extracted peptides were dried and subsequently resuspended in a water:acetonitrile:formic acid solution with a ratio of 95:3:2, in preparation for LC-MS/MS (Liquid Chromatography with tandem mass spectrometry) analysis. This analysis was performed using a Dionex Ultimate 3000 UHPLC system coupled to a high-resolution Q Exactive mass spectrometer (Thermo Scientific, Bremen, Germany), housed at the "Centro Interdipartimentale Grandi Strumenti" of the University of Modena and Reggio Emilia. Each sample underwent a 60-min run time. An inclusion list featuring the peptides of interest was incorporated into the method, with m/z values of [M + 2H]+2523.7748; 440.2233; 540.2796; 525.2975; 575.7533; and 656.3528. A comprehensive description of the analytical protocol can be found in Lugli et al. (2019b, 2020).

Xcalibur™ (Thermo Scientific) was used to manually examine ion chromatograms, specifically searching for AMELX and AMELY peptides, as outlined by Stewart et al. (2017) and Lugli et al. (2019b). Raw data were converted into Mascot generic format (MsConvert v. 3.0.10730, ProteoWizard tools) to refine sex estimation and potentially identify other endogenous tooth proteins. This data was then cross-referenced against: 1) the Swiss-Prot database (restricted to *Homo sapiens*); 2) an in-house database sourced from UniProt & NCBI, encompassing all available mammalian amelogenin sequences; and 3) the cRAP database, which contains 116 sequences, for potential contaminants. The search parameters mirrored those of (Lugli et al., 2020). A protein was deemed identified if a minimum of two distinct significant peptides were observed. Raw MS data were deposited in Zenodo (10.5281/zenodo.15387116).

2.7. Radiocarbon analysis

Approximately 250 mg of the infant's remaining bone fragments were prepared for AMS (Accelerator Mass Spectrometry) radiocarbon dating at the Centre of Applied Physics, Dating, and Diagnostics, Department of Mathematics and Physics "Ennio de Giorgi", University of Salento (Calcagnile et al., 2019). Macrocontaminants were identified under optical microscopy and removed mechanically. The bone fragments were then powdered using a pestle and mortar, demineralised in 1 % HCl at room temperature, and gelatinized in acidified water (HCl, pH = 3) at 85 °C (Longin, 1971). The resulting gelatin was filtered through 0.45 μm pore silver filters. The extraction yield was <0.1 %, indicating insufficient collagen preservation and extensive diagenesis, which ultimately prevented radiocarbon dating of the sample.

3. Results

3.1. Anthropological analysis

The excavation of the remains revealed their fragmentary nature, with only some dental crowns being recovered intact. In the maxillary arch, the deciduous dentition was mostly retrieved (though many were in poor condition, with eroded roots and often damaged cervix), except for the first and second left deciduous incisors. The permanent dentition in the maxillary arch, still in crown formation, includes central and lateral incisors and both first molars. In the mandibular arch, the entire deciduous dentition is present. The permanent dentition, also in crown formation, includes the central incisors and the right first molar (Supplementary Fig. 1). Based on the observed dental development stage, reported in Supplementary Table 1, the infant's age at death is estimated to be approximately between 1.5 and 2.5 years (AlQahtani et al., 2010). No hypoplastic defects or carious lesions were visible on the dentition.

3.2. Histological analysis

Analysis of the histological thin section of the URdm[1] (Fig. 3) reveals a distinct neonatal line, whereas no accentuated line (AL; indicators of physiological stress events in enamel) was detected. Crown growth parameters (Table 1) display a mean inner enamel DSR (within 100 μm from the EDJ) across the EDJ's length of 3.13 ± 0.17 $\mu m d^{-1}$ (n = 176) on the paracone and of 3.21 ± 0.21 $\mu m d^{-1}$ (n = 159) on the protocone, ranging from 2.61 $\mu m d^{-1}$ to 3.69 $\mu m d^{-1}$. For both cusps, there is no significant difference in DSR averages between cuspal and imbricational inner enamel (Supplementary Table 2).

Enamel extension rate (EER) during the first ~30-days of cusp formation is estimated at 51.22 $\mu m d^{-1}$ on the paracone and 44.38 $\mu m d^{-1}$ on the protocone, gradually decelerating during subsequent development, but with a transient surge following birth. Overall, the mean EER of the crown, based on the paracone, can be estimated at 15.20 $\mu m d^{-1}$.

Based on the paracone – which is the cusp encompassing the complete formation of the tooth since the thin section's plane was centred according to its dentine horn – CFT was estimated at ~374 days. The position of the NNL enables the distinction between the prenatal and postnatal formation of the crown, estimating crown initiation (Ci) at

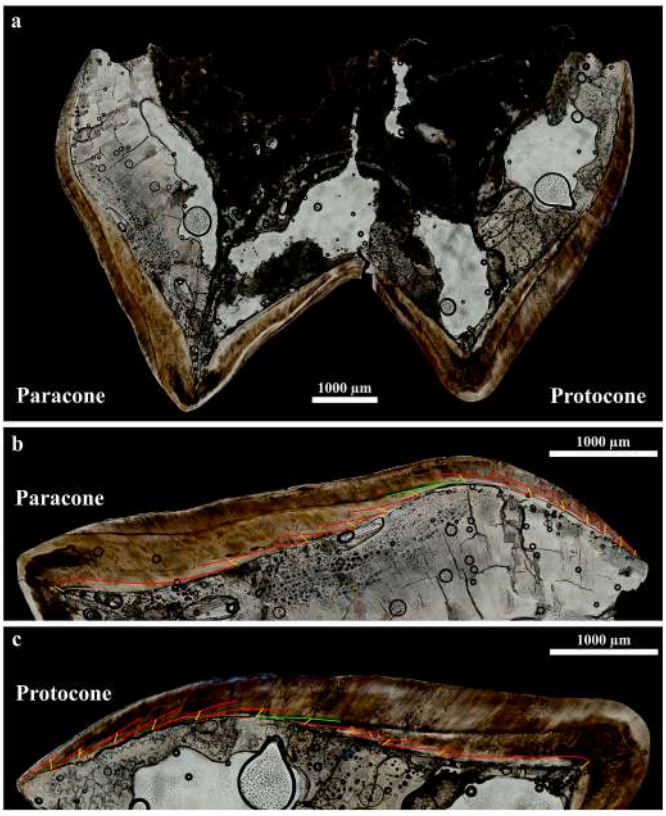

Fig. 3. Histological thin section and magnified views of the URdm1 for chronological analysis. (a) Histological thin section of the upper right deciduous first molar (URdm1), showing the paracone (left) and protocone (right). (b) Magnified view of the paracone. (c) Magnified view of the protocone. The color-coded lines in the magnified panels illustrate key microstructural markers utilized for chronological mapping: green represents the neonatal line (NNL), red denotes isochronous Retzius lines, and orange highlights the selected prism segments used for the chronological reconstruction. Scale bars = 1000 µm. (For interpretation of the references to color in this figure legend, the reader is referred to the Web version of this article.)

Table 1
Crown growth and developmental parameters of paracone and protocone aspects of the URdm[1] and of the LRM1's protoconid. DSR (daily secretion rate), EER (enamel extension rate), Ci (crown initiation), Crc (crown completion), CFT (crown formation time). † From average timing in literature (AlQahtani et al., 2010; Hillson, 1996; Antoine et al., 2009; Reid et al., 1998). * Crown not complete as it was still in formation at the moment of death.

		URdm1		LRM1
		Paracone	Protocone	Protoconid
DSR (μmd^{-1})	Min	2.68	2.61	2.72
	Max	3.69	3.66	3.24
	Mean	3.13	3.21	2.97
	sd	0.17	0.21	0.12
	n	176	159	113
EER (μmd^{-1})	Min	4.95	4.63	2.57
	Max	51.22	44.38	60.18
	Mean	15.20	16.69	8.17
Ci (days)		−184	NA	Birth†
Crc (days)		189	190	NA
CFT (days)		374	NA	505*

~184 days before birth and crown completion (Crc) at ~189 days after birth. For the protocone, Ci remains indeterminate due to section orientation (i.e. the thin section does not encompass its dentine horn), whereas Crc was estimated at ~190 days.

In addition, the position of the NNL within the crown of the tooth (Fig. 3) denotes that the crown was at the Cr ¾ stage of formation (Moorrees et al., 1963b) at the time of birth.

On the other hand, the histological thin section of the LRM_1 (Fig. 4) lacks a manifest NNL or any evident AL. Crown growth parameters (Table 1), measured on the protoconid, exhibit a mean inner enamel (within 100 µm from the EDJ) DSR across the EDJ's length of 2.97 ± 0.12 μmd^{-1} (n = 113), ranging from 2.72 μmd^{-1} to 3.24 μmd^{-1}. As the crown was still in formation and had just started the formation of imbricational enamel, a distinction between cuspal and imbricational inner enamel DSRs was not carried out.

EER during the first ~30-day period of protoconid formation is estimated at 60.18 μmd^{-1}, with values decreasing as the tooth develops. The overall mean EER of the cusp is estimated at 8.17 μmd^{-1} (Table 1).

The absence of a clear NNL (Fig. 4) prompted the alignment of Ci with birth based on literature references (AlQahtani et al., 2010; Hillson, 1996; Reid and Dean, 2006). The incomplete crown formation of the LRM_1 prevents a total CFT estimation. However, the cessation of enamel secretion at ~505 days does inform on an estimate age at death of ~74 weeks (i.e. ~17 months) from birth, after accounting for a minimum of 14 additional days due to the loss of the last formed immature enamel (Antoine et al., 2009).

3.3. Trace element analysis

Spatially-resolved geochemical analyses were conducted by LA-

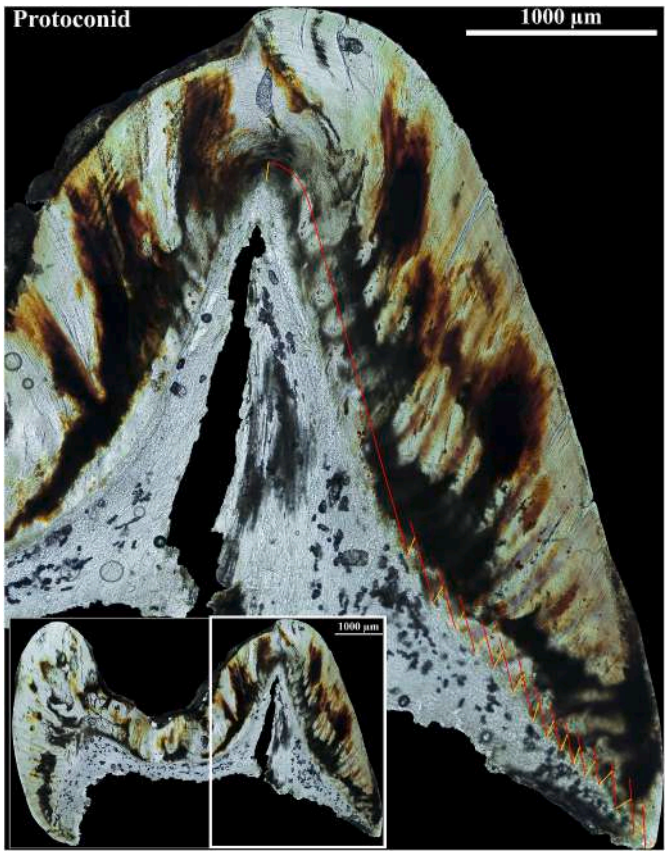

Fig. 4. Histological thin section of the lower right first molar (LRM1). The inset image on the bottom left depicts the full thin section, showing the protoconid (right) and metaconid (left), while the larger image is a magnified view of the protoconid, indicated by the white frame. The magnified section highlights key microstructural features used for chronological mapping: red lines denote isochronous Retzius lines, and orange lines mark the selected prism segments used for chronological reconstruction. Scale bars = 1000 µm. (For interpretation of the references to color in this figure legend, the reader is referred to the Web version of this article.)

ICPMS on both the buccal and lingual aspects of the URdm[1]. The trace element analysis targeted uranium (U), manganese (Mn), and lead (Pb) as primary diagenetic proxies, alongside strontium-to-calcium (Sr/Ca) and barium-to-calcium (Ba/Ca) ratios, which under ideal preservation conditions can provide biogenic information regarding diet and nursing behaviours. The elemental profiles of both aspects (Fig. 5; Supplementary Fig. 2; Supplementary Table 3) exhibited a pronounced diagenetic overprint, evinced by generally elevated concentrations of uranium (U) and manganese (Mn) (Grimstead et al., 2018; Müller et al., 2024; Willmes et al., 2016).

On the buccal aspect, U concentrations along the EDJ path are particularly elevated in the pre-natal portion of enamel and during the first ~20 days post-birth (ranging between ~0.48 μg/g and ~23.36 μg/g). Conversely, the enamel portion following the first ~20 days post-birth exhibited relatively lower and more constant uranium concentrations (~0.23 μg/g on average), which remain however high. On the other hand, manganese concentrations gradually decrease throughout prenatal enamel up to the first ~20 days after birth, to then start increasing again at ~50 days post-birth. This post-natal pattern is also observed in lead (Pb) concentrations, which remain low and constant in the pre-natal portion, and mimic Mn and U in the post-natal portion (Fig. 5). The strontium-to-calcium ratio (Sr/Ca) presents little variation along the buccal EDJ path (~6.67e-4 μg/g on average), whereas the barium-to-calcium ratio (Ba/Ca) exhibits greater variation. Both profiles present remarkable correlation with both U and Mn profiles, suggesting post-depositional mobilisation of these elements and hence diagenetic overprinting masking the original biogenic signal (Fig. 5).

On the lingual aspect, U concentrations are also generally elevated (~5.3 μg/g on average) along most of the EDJ path, with a relative decrease observed from ~150 days post-birth onwards. On the other hand, Mn concentrations are particularly elevated in the pre-natal portion, showing a relative decline in the post-natal portion (~15.09 μg/g on average). In contrast, lead (Pb) concentrations on the lingual EDJ path were generally low, averaging ~0.14 μg/g (Fig. 5). The overall elevated concentrations of diagenetic proxy elements suggest widespread diagenetic overprinting also on this aspect. Both Sr/Ca (~6.70e-4 μg/g on average) and Ba/Ca (~1.63e-4 μg/g on average) ratios exhibit slight variations along the lingual EDJ path correlating with both U and Mn profiles (Fig. 5), pointing towards post-depositional elemental influxes likely masked the original biogenic signal, compromising the possibility of reliable dietary reconstruction.

3.4. Genomic analysis

The sample reported a low presence of endogenous DNA after whole genome sequencing, with only 1006 fragments out of more than 6 million being of human origin. This resulted in ultra-low coverage along the nuclear genome, with only 0.008 % of the genome covered by at least one sequence. By contrast, mitochondrial DNA capture resulted in 1779 unique reads mapping to the mitochondrial reference sequence, and 96 % of the entire mitochondrial genome was covered by at least 2 reads. The observed fragments of DNA were investigated for authenticity through DamageProfiler, which reported weak evidence of degradation among the most extreme bases of the reads mapped to the nuclear genome due to the low coverage nature of the shotgun sequencing (Fig. 6a), while results of degradation patterns are more robust on mitochondrial DNA, and consistent with the age of the sample (Fig. 6b). Despite the low presence of endogenous nuclear DNA from the

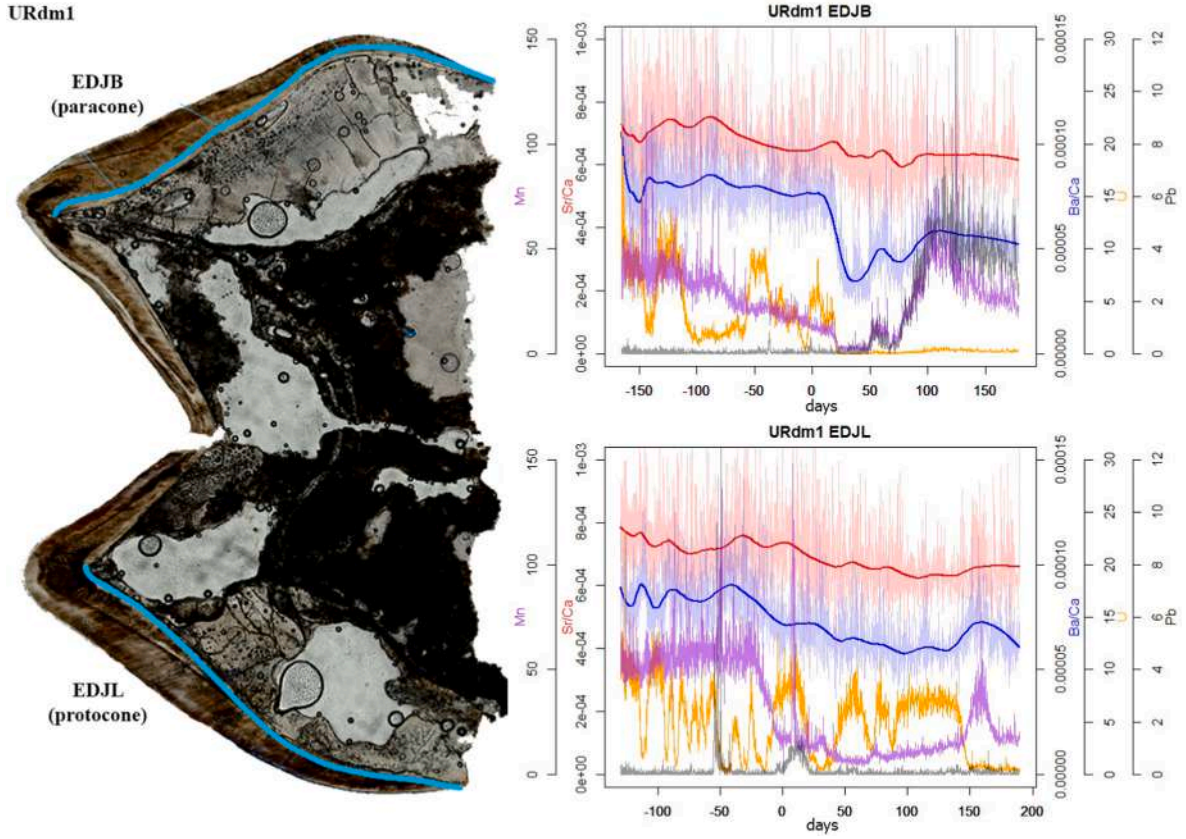

Fig. 5. Trace element profiles of Sr/Ca, Ba/Ca, U, Mn, and Pb measured along the enamel-dentine junction of the upper right deciduous first molar (URdm1), from both the buccal aspect (paracone) and lingual aspect (protocone). The picture on the left displays the histological section of the URdm1, with the laser ablation tracks highlighted in light blue. The profiles on the right represent the trace element distributions, with the paracone (EDJB) shown in the top graph and the protocone (EDJL) in the bottom graph. The trace elements include Sr/Ca (red), Ba/Ca (blue), U (purple), Mn (yellow), and Pb (grey). The X-axis represents days of life, with 0 representing birth. (For interpretation of the references to color in this figure legend, the reader is referred to the Web version of this article.)

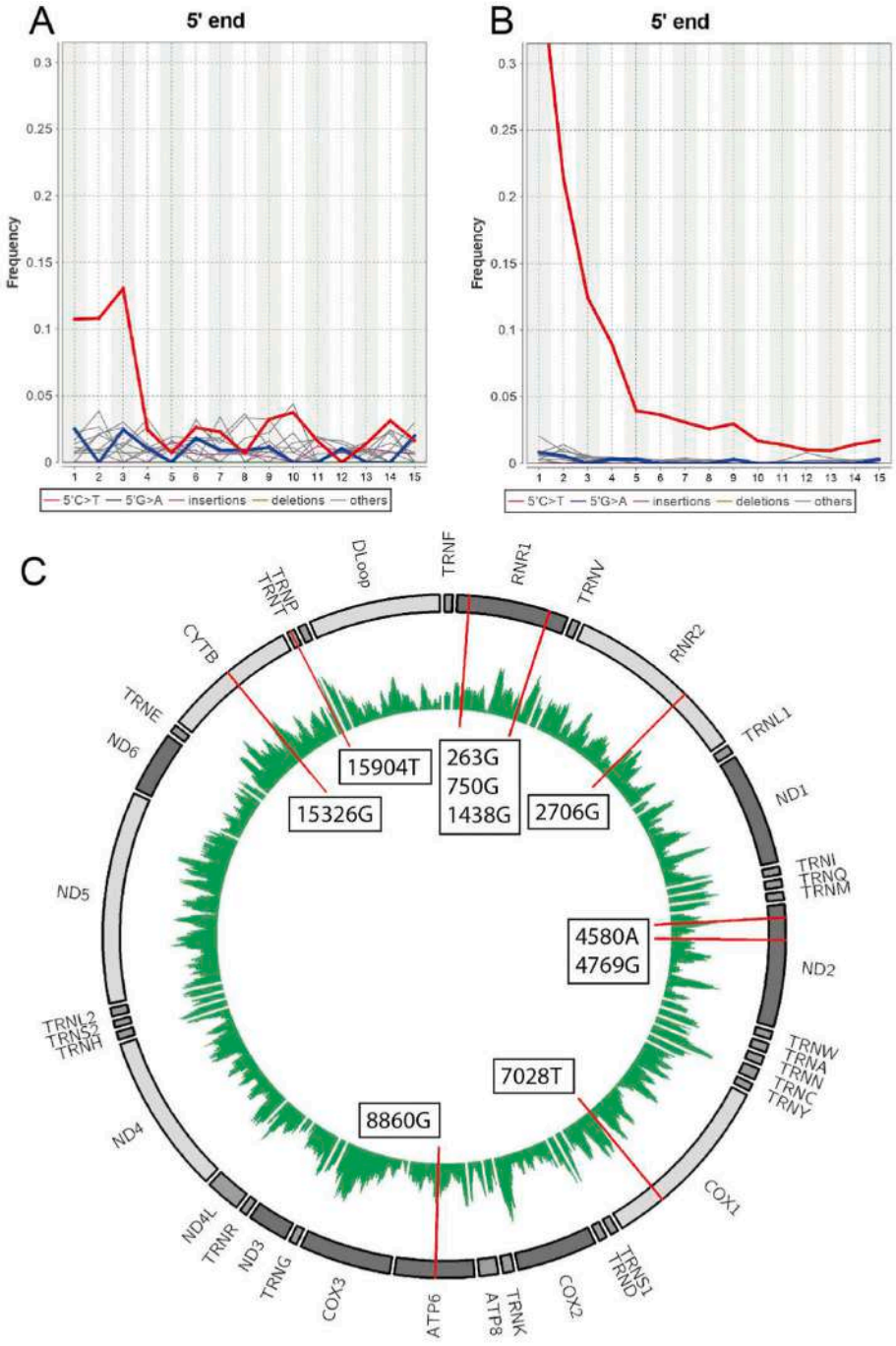

Fig. 6. Deamination patterns on 5′ end of ancient DNA fragments after shotgun sequencing (a) and mitochondrial DNA capture enrichment (b). The reconstructed mitochondrial genome (c) with coverage at each position marked by green bars, and haplogroup defining variants. (For interpretation of the references to color in this figure legend, the reader is referred to the Web version of this article.)

individual, we tentatively investigated the biological sex of the infant. By computing the ratio of sequences that aligned to the X-chromosome as a portion of the sequences mapping to the autosomes (Mittnik et al., 2016), the sample resulted to be consistent with the assignment of biological sex as male, with Rx ~0.563 (95 % CI 0.501–0.624).

To validate the authenticity of the retrieved DNA we estimated contamination on mitochondrial sequences using Schmutzi (Renaud et al., 2015), that allows to calculate the frequency of deamination at the 5′ and 3' ends of the reads, and to compare the reconstructed endogenous sequence with a dataset of possible contaminating mitogenomes. Both the analyses reported an estimate of contamination ~1 %, indicating absence of modern sources of contamination at the mitochondrial level. We compared the consensus sequence reconstructed by Schmutzi with the original BAM files in IGV and detected 10 informative variants (263G, 750G, 1438G, 2706G, 4580A, 4769G, 7028T, 8860G, 15236G, 15904T) that were used as input in Haplogrep3, leading to the assignment of the mitochondrial haplogroup V+@72, a sub-clade of V that lost the known diagnostic substitution T72C located in the HVS-II region (Fig. 6c).

3.5. Proteomic analysis

Following the examination of ion chromatograms, both peptides SIRPPYPSY, associated with the AMELX gene, and SM(ox)IRPPY, linked

to the AMELY gene, were identified. A pronounced ion signal of ~4.5e6 was associated with the AMELY specific peptide (Fig. 7), confirming the male sex of the infant from Faenza. No modern contaminants were identified through queries in the cRAP database.

3.6. Radiocarbon analysis

Radiocarbon analysis was attempted on the sample; however, it was found to be undatable due to an insufficient collagen content. The low collagen yield following pretreatment indicated a level of degradation that prevented reliable radiocarbon dating, thus precluding further chronological information from this sample.

4. Discussions

The suboptimal preservation of skeletal remains can often hinder the biological reconstruction of archaeological and fossil records, consequently restricting detailed analysis of the respective contexts and populations. In this study, the pronounced deterioration of the skeletal remains has unequivocally led to a substantial loss of biological information. The sole informative anatomical elements to have survived are the dental crowns, which only provided an estimate of the infant's age at death – approximately 1.5 years of age, based on contemporary established standards (AlQahtani et al., 2010; Hillson, 1996). Nevertheless, the implementation of advanced bioanthropological analyses has enabled the extraction of further biological data that might otherwise have remained unobserved.

The microscopic analysis of the dental enamel of the URdm^1 and LRM$_1$ provided detailed insight into the infant's development and early life history, refining the age at death estimate to approximately 74 weeks (i.e. ~17 months), considering a minimum of 14 additional days for the loss of the last formed immature enamel (Antoine et al., 2009). From a biorhythmic perspective, the mean inner enamel DSR for the deciduous molar (URdm1) – 3.13 ± 0.17 μmd^{-1} (n = 176) for the paracone and 3.21 ± 0.21 μmd^{-1} (n = 159) for the protocone (Table 1) – aligns with values recorded in Italian Early Medieval populations (Magri et al., 2024). In contrast, these rates are lower than the averages documented for British Bronze age and Mediaeval populations (Mahoney, 2011) and for a contemporary global population (McFarlane et al., 2021), though they remain within established ranges (Birch and Dean, 2009; Mahoney, 2015; McFarlane et al., 2021). Notably, contrary to findings by McFarlane et al. (2021), minimal variation between the cuspal and imbricational enamel within both cusps was identified in this individual (Supplementary Table 2). Furthermore, the mean inner enamel DSR for the permanent molar (LRM$_1$) – 2.97 ± 0.12 μmd^{-1} (n = 113) (Table 1) – correlates well with previously reported values (Aris, 2022; Mahoney, 2008). EERs, often underrepresented in the literature (Mahoney, 2015), were employed to ascertain the rate of new enamel secretion along the EDJ, reflecting the crown's longitudinal growth rate. Comparative analysis between the two crowns indicated, as expected, that the mean EER for the deciduous molar's paracone (14.5 μmd^{-1}) exceeds that of the permanent molar (8.2 μmd^{-1}). However, the initial EER for the first approximately 30 days of crown formation was marginally slower for the deciduous molar (51.2 μmd^{-1}) compared to the permanent molar (60.2 μmd^{-1}) (Table 1). Mean EERs align with the few available published averages, whereas initial EERs are notably higher (Higgins et al., 2024; Mahoney, 2015; Smith et al., 2010), partly due to the shorter time interval used in this study for calculating initial EERs.

Total CFTs of both dental specimens, considering their respective stages of development, are consistent with the durations reported in the literature for each dental class (Dean et al., 1993a; Magri et al., 2024; Mahoney, 2008, 2015; Reid et al., 1998; Reid and Dean, 2006; Smith et al., 2010). However, the estimated Ci of the URdm^1's paracone occurs relatively early when compared to published data for the same cusp (Mahoney, 2015). Accordingly, the estimated time at Crc falls within the earlier range of the variability reported for modern European populations (AlQahtani et al., 2010; Hillson, 1996). Additionally, the position of the NNL within the tooth corroborates its advanced stage of formation at birth (Cr ¾; Moorrees et al., 1963b) compared to contemporary European standards (AlQahtani et al., 2010; Hillson, 1996).

For the LRM$_1$, in the absence of a discernible NNL, Ci was aligned with birth, adhering to the convention in the literature (e.g. (Beynon et al., 1998; Higgins et al., 2024; Reid and Dean, 2006),). The stage of formation at ~505 days (~Cr ½; Moorrees et al., 1963b) places it at a comparatively advanced stage of development by modern standards (AlQahtani et al., 2010), although the completion of the cusp (Table 1) aligns with averages reported for modern northern Europeans (Reid and Dean, 2006).

The lack of discernible accentuated lines (physiological stress markers; Nava et al., 2019; Wilson and Shroff, 1970) in both prenatal and postnatal enamel suggests generally good health conditions for the mother during gestation (prenatal portion of the URdm^1; see Nava et al., 2017b) and the infant after birth. Nevertheless, the infant's early demise (~17 months of age) is noted.

Taken together, the dental histological data offer a refined and multidimensional perspective on the individual's developmental trajectory and early life history. They also contribute to broader discussions on human growth physiology and population-level variability, underscoring how archaeological populations may diverge from modern

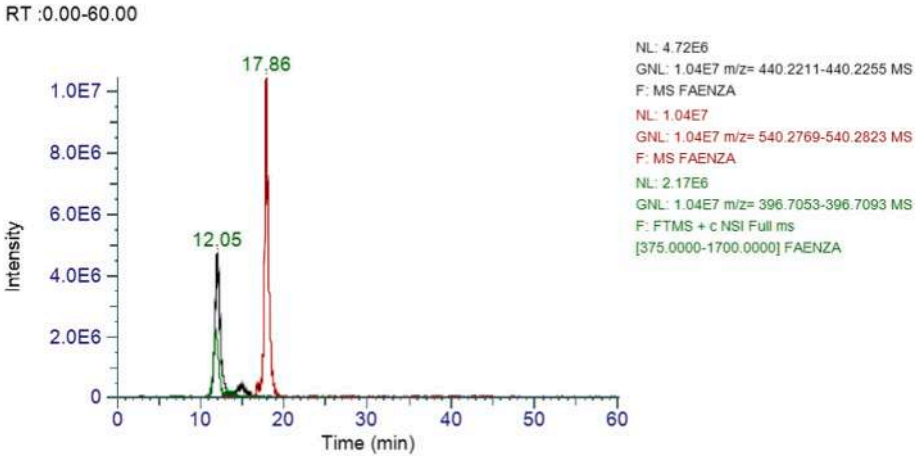

Fig. 7. Chromatogram portraying the peaks identifying the presence of AMELX and AMELY specific peptides. The black peak is peptide SM(ox)IRPPY (AMELY; [M + 2 H]+2440.2233 m/z); the green peak is peptide M(ox)IRPPY (AMELY; [M + 2 H]+2396.7073 m/z); while the red peak is peptide SIRPPYPSY (AMELX; [M + 2 H]+ 2540.2796 m/z). (For interpretation of the references to color in this figure legend, the reader is referred to the Web version of this article.)

reference standards commonly used in developmental estimations.As might be expected given the poor physical preservation of the remains, high levels of diagenetic overprinting have precluded reliable investigations into dietary shifts or potential exposure to pollutants. Under good preservation conditions, Sr/Ca and Ba/Ca profiles in dental tissues are frequently used to assess breastfeeding, weaning, and other dietary transitions (Austin et al., 2013; Müller et al., 2019b; Nava et al., 2020, 2024; Smith et al., 2018). In this case, however, the correlation between these dietary proxies and diagenetic indicators such as U and Mn suggests that post-depositional elemental influxes have likely masked the original biogenic signals. This diagenetic alteration prevents distinguishing, in the affected portions, whether variations in elemental concentrations reflect physiological processes or diagenetic contamination (Higgins et al., 2024; Nava et al., 2020; Willmes et al., 2016). Furthermore, the diagenetic proxies present variating profiles, indicative of differential diagenetic impacts on the pre- and post-natal portions of the deciduous molar's crown, further limiting the interpretive reliability of the data.

Despite the presence of diagenetic biogeochemical alterations within the enamel, proteomic analysis of the tissue remained unaffected, unambiguously identifying the sex of the infant as male. Meanwhile, attempts at radiocarbon dating were unsuccessful due to the insufficient collagen content in the bone fragments, limiting our ability to anchor the findings within a precise chronological framework.

On the other hand, despite the scarce preservation of endogenous material, the genomic analysis successfully identified the infant's sex as male, confirming the attribution obtained through amelogenin analysis, and provided insights into his matrilineal descent by the almost complete reconstruction of the mitochondrial genome. Notably, the infant reports an uncommon mtDNA haplogroup - V+@72 - which is attested in the literature only in one other ancient sample from the Eneolithic necropolis of Serra Cabriles, in north-western Sardinia (Fernandes et al., 2018), and dated to 2454-2201 cal BCE. The V+@72 haplotype belongs to the V sub-haplogroup, a minor branch of the HV0 clade, which is relatively rare among modern Europeans and has high frequencies recorded only in the Saami population of northern Fenno-Scandinavia (Tambets et al., 2004). A likely western Mediterranean origin of this haplogroup during the Last Glacial Maximum has been suggested (Secher et al., 2014; Torroni et al., 1998), with V-related haplotypes sporadically encountered during the Eneolithic in Iberia and central Europe (Olalde et al., 2018, 2019; Villalba-Mouco et al., 2021). Due to the low coverage nature of the sample, it was not possible to perform genome-wide inferences, and future paleogenetic data will be essential to investigate the genetic make-up of Eneolithic communities in Adriatic Italy.

Overall, given that the infant remains were found isolated, with scant contextual information, it is not possible to ascribe the reconstructed biological and ancestral characteristics to the broader local population, necessitating further comprehensive investigation into the local groups residing in the area at that time. Nevertheless, the present study demonstrates how the integration of advanced bioanthropological techniques can overcome the interpretive limitations typically imposed by poorly preserved osteological material. Dental histology enabled the high-resolution estimation of age at death and provided insights into developmental dynamics through enamel growth parameters. Although biogeochemical analysis was compromised by diagenetic alteration, the assessment of post-depositional contamination itself proved essential for evaluating the reliability of dietary reconstructions and should be considered a fundamental part of such investigations. Proteomic analysis of enamel peptides and palaeogenomic investigation of osseous fragments jointly confirmed the sex of the infant as male and contributed mitochondrial haplogroup data, revealing an uncommon maternal lineage within Eneolithic Italy. Together, these findings underscore the potential of a multidisciplinary approach to recover meaningful biological and genetic information, even from highly fragmentary skeletal material, illustrating that isolated remains need not remain silent.

CRediT authorship contribution statement

Owen Alexander Higgins: Writing – review & editing, Writing – original draft, Visualization, Project administration, Investigation, Formal analysis, Data curation, Conceptualization. **Francesco Fontani:** Writing – review & editing, Writing – original draft, Visualization, Project administration, Investigation, Formal analysis, Data curation, Conceptualization. **Federico Lugli:** Writing – review & editing, Formal analysis, Data curation. **Sara Silvestrini:** Writing – review & editing, Visualization, Investigation, Formal analysis, Data curation. **Antonino Vazzana:** Writing – review & editing, Investigation. **Adriana Latorre:** Writing – review & editing, Investigation. **Massimo Sericola:** Writing – review & editing, Investigation. **Anna Cipriani:** Writing – review & editing, Resources. **Gianluca Quarta:** Writing – review & editing, Resources. **Lucio Calcagnile:** Writing – review & editing, Resources. **Luca Bondioli:** Writing – review & editing, Supervision, Software. **Alessia Nava:** Writing – review & editing, Supervision. **Elisabetta Cilli:** Writing – review & editing, Supervision. **Donata Luiselli:** Writing – review & editing, Supervision, Resources, Funding acquisition. **Stefano Benazzi:** Writing – review & editing, Resources, Project administration, Funding acquisition, Conceptualization.

Data availability statement

The data that support the findings of this study are included as part of the paper and supplementary materials or available in European Nucleotide Archive under project accession number PRJEB89577, and Zenodo at 10.5281/zenodo.15387116.

Declaration of competing interest

The authors declare that they have no known competing financial interests or personal relationships that could have appeared to influence the work reported in this paper.

Acknowledgements

We thank the Soprintendenza Archeologia, Belle Arti e Paesaggio per le province di Ravenna, Forlì-Cesena e Rimini for its availability and for granting the permissions to perform the various analyses for this study. We also extend our gratitude to Impresa Edile Santucci Costruzioni S.r.l. and Gruppo Ritmo S.r.l. for their cooperation and support during the discovery and excavation of the remains. Special thanks to Professor Claudio Cavazzuti for his expert analysis of the ceramic sherds, which confirmed a probable Eneolithic chronology.

Alessia Nava received funding from the European Research Council (ERC) under the European Union's Horizon Europe Research and Innovation Programme (GA no. 101077348 — MOTHERS; https://erc-mothers.eu/).

The paleogenomic analyses were sustained by the MIUR-PRIN 20177PJ9XF granted to Donata Luiselli.

AC received financial support from the European Union - NextGenerationEU - National Recovery and Resilience Plan (NRRP) – MISSION 4 COMPONENT 2, INVESTIMENT N. 1.1, CALL PRIN 2022 PNRR D.D. 1409 14-09-2022 – "CAST Copper Accumulation, Supply, and Technology among Italian prehistoric societies", Codice progetto: P202275A2M, Decreto di finanziamento MUR D.D. n. 1388 del 1 settembre 2023 (CUP N. E53D23020120001).

Appendix A. Supplementary data

Supplementary data to this article can be found online at https://doi.org/10.1016/j.jas.2025.106291.

References

AlQahtani, S.J., Hector, M.P., Liversidge, H.M., 2010. Brief communication: the London atlas of human tooth development and eruption. Am. J. Phys. Anthropol. 142, 481–490. https://doi.org/10.1002/ajpa.21258.

Antoine, D., Hillson, S., Dean, M.C., 2009. The developmental clock of dental enamel: a test for the periodicity of prism cross-striations in modern humans and an evaluation of the most likely sources of error in histological studies of this kind. J. Anat. 214, 45–55. https://doi.org/10.1111/J.1469-7580.2008.01010.X.

Aris, C., 2022. Enamel growth rate variation of inner, mid, and outer enamel regions between select permanent tooth types across five temporally distinct British samples. Arch. Oral Biol. 137. https://doi.org/10.1016/j.archoralbio.2022.105394.

Austin, C., Smith, T.M., Bradman, A., Hinde, K., Joannes-Boyau, R., Bishop, D., Hare, D. J., Doble, P., Eskenazi, B., Arora, M., 2013. Barium distributions in teeth reveal early-life dietary transitions in primates. Nature 498, 216–219. https://doi.org/10.1038/nature12169.

Bagolini, B., 1984. Il Neolitico e l'età del Rame Documentazione dei resti culturali. Archeologia a Spilamberto 27–95.

Bagolini, B., 1981. Il Neolitico e l'età del rame. In: Ricerca a Spilamberto - S. Cesario 1977-1980. Cassa di Risparmio di Vignola.

Bello, S.M., Thomann, A., Signoli, M., Dutour, O., Andrews, P., 2006. Age and sex bias in the reconstruction of past population structures. Am. J. Phys. Anthropol. 129, 24–38. https://doi.org/10.1002/ajpa.20243.

Beynon, A.D., Dean, M.C., Leakey, M.G., Reid, D.J., Walker, A., 1998. Comparative dental development and microstructure of Proconsul teeth from Rusinga Island, Kenya. J. Hum. Evol. 35, 163–209. https://doi.org/10.1006/jhev.1998.0230.

Birch, W., Dean, M.C., 2009. Rates of enamel formation in human deciduous teeth. In: Frontiers of Oral Biology. Front Oral Biol, pp. 116–120. https://doi.org/10.1159/000242402.

Birch, W., Dean, M.C., 2014. A method of calculating human deciduous crown formation times and of estimating the chronological ages of stressful events occurring during deciduous enamel formation. J. Forensic Leg. Med. 22, 127–144. https://doi.org/10.1016/j.jflm.2013.12.002.

Boutin, A.T., 2022. Osteobiography and Case Studies. The Routledge Handbook of Paleopathology, pp. 192–209. https://doi.org/10.4324/9781003130994-12.

Budd, P., Montgomery, J., Evans, J., Trickett, M., 2004. Human lead exposure in England from approximately 5500 BP to the 16th century AD. Sci. Total Environ. 318, 45–58. https://doi.org/10.1016/S0048-9697(03)00357-7.

Calcagnile, L., D'Elia, M., Maruccio, L., Braione, E., Celant, A., Quarta, G., 2019. Solving an historical puzzle: radiocarbon dating the Capitoline she wolf. Nucl. Instrum. Methods Phys. Res. B 455, 209–212. https://doi.org/10.1016/j.nimb.2019.01.008.

Cilli, E., 2024. Archaeogenetics. In: Encyclopedia of Archaeology, second ed. Elsevier, pp. 1038–1047. https://doi.org/10.1016/B978-0-323-90799-6.00017-3.

Cleveland, W.S., Grosse, E., Shyu, W.M., 1992. Local regression models. In: Chambers, J. M., Hastie, T.J. (Eds.), Statistical Models in S. Routledge. https://doi.org/10.1201/9780203738535-8.

Cocchi Genick, D., 2009. Preistoria. QuiEdit.

Dabney, J., Knapp, M., Glocke, I., Gansauge, M.T., Weihmann, A., Nickel, B., Valdiosera, C., García, N., Pääbo, S., Arsuaga, J.L., Meyer, M., 2013. Complete mitochondrial genome sequence of a Middle Pleistocene cave bear reconstructed from ultrashort DNA fragments. Proc. Natl. Acad. Sci. U. S. A. 110, 15758–15763. https://doi.org/10.1073/pnas.1314445110.

Danecek, P., Bonfield, J.K., Liddle, J., Marshall, J., Ohan, V., Pollard, M.O., Whitwham, A., Keane, T., McCarthy, S.A., Davies, R.M., 2021. Twelve years of SAMtools and BCFtools. GigaScience 10. https://doi.org/10.1093/gigascience/giab008.

Dean, C., 2017. How the microstructure of dentine can contribute to reconstructing developing dentitions and the lives of hominoids and hominins. C. R. Palevol 16, 557–571. https://doi.org/10.1016/j.crpv.2016.10.006.

Dean, M.C., 2012. Daily rates of dentine formation and root extension rates in Paranthropus boisei , KNM-ER 1817, from Koobi Fora, Kenya. In: African Genesis. Cambridge University Press, pp. 268–279. https://doi.org/10.1017/cbo9781139096164.017.

Dean, M.C., 1987. Growth layers and incremental markings in hard tissues; a review of the literature and some preliminary observations about enamel structure in Paranthropus boisei. J. Hum. Evol. https://doi.org/10.1016/0047-2484(87)90074-1.

Dean, M.C., Beynon, A.D., Reid, D.J., Whittaker, D.K., 1993a. A longitudinal study of tooth growth in a single individual based on long- and short-period incremental markings in dentine and enamel. Int. J. Osteoarchaeol. 3, 249–264. https://doi.org/10.1002/oa.1390030404.

Dean, M.C., Beynon, A.D., Thackeray, J.F., Macho, G.A., 1993b. Histological reconstruction of dental development and age at death of a juvenile Paranthropus robustus specimen, SK 63, from Swartkrans, South Africa. Am. J. Phys. Anthropol. 91, 401–419. https://doi.org/10.1002/ajpa.1330910402.

Dirks, W., 1998. Histological reconstruction of dental development and age at death in juvenile gibbon (Hylobates lar). J. Hum. Evol. 35, 411–425. https://doi.org/10.1006/jhev.1997.0185.

Ewels, P., Magnusson, M., Lundin, S., Käller, M., 2016. MultiQC: summarize analysis results for multiple tools and samples in a single report. Bioinformatics 32, 3047–3048. https://doi.org/10.1093/bioinformatics/btw354.

Fellows Yates, J.A., Lamnidis, T.C., Borry, M., Valtueña, A.A., Fagernäs, Z., Clayton, S., Garcia, M.U., Neukamm, J., Peltzer, A., 2021. Reproducible, portable, and efficient ancient genome reconstruction with nfcore/eager. PeerJ 9. https://doi.org/10.7717/peerj.10947.

Fernandes, D.M., Strapagiel, D., Borówka, P., Marciniak, B., Żądzińska, E., Sirak, K., Siska, V., Grygiel, R., Carlsson, J., Manica, A., Lorkiewicz, W., Pinhasi, R., 2018. A genomic Neolithic time transect of hunter-farmer admixture in central Poland. Sci. Rep. 8. https://doi.org/10.1038/s41598-018-33067-w.

Fontani, F., Boano, R., Cinti, A., Demarchi, B., Sandron, S., Rampelli, S., Candela, M., Traversari, M., Latorre, A., Iacovera, R., Abondio, P., Sarno, S., Mackie, M., Collins, M., Radini, A., Milani, C., Petrella, E., Giampalma, E., Minelli, A., Larocca, F., Cilli, E., Luiselli, D., 2023. Bioarchaeological and paleogenomic profiling of the unusual Neolithic burial from Grotta di Pietra Sant'Angelo (Calabria, Italy). Sci. Rep. 13, 1–15. https://doi.org/10.1038/s41598-023-39250-y.

Grimstead, D.N., Clark, A.E., Rezac, A., 2018. Uranium and vanadium concentrations as a trace element method for identifying diagenetically altered bone in the inorganic phase. J. Archaeol. Method Theor 25, 689–704. https://doi.org/10.1007/s10816-017-9353-z.

Grün, R., Aubert, M., Joannes-Boyau, R., Moncel, M.H., 2008. High resolution analysis of uranium and thorium concentration as well as U-series isotope distributions in a Neanderthal tooth from Payre (Ardèche, France) using laser ablation ICP-MS. Geochem. Cosmochim. Acta 72, 5278–5290. https://doi.org/10.1016/J.GCA.2008.08.007.

Grupe, G., 2007. Taphonomic and diagenetic processes. In: Henke, W., Tattersall, I. (Eds.), Handbook of Paleoanthropology: Vol I: Principles, Methods and Approaches. Springer.

Higgins, O.A., Lugli, F., Mianowski, S., Galbusera, A., Anczkiewicz, R., Benazzi, S., Müller, W., Nava, A., Bondioli, L., 2025. Timewise registration of histomorphometric and biogeochemical data in human dental mineralized tissues through LOESS regression). Conference Proceedings.

Higgins, O.A., Modi, A., Cannariato, C., Diroma, M.A., Lugli, F., Ricci, S., Zaro, V., Vai, S., Vazzana, A., Romandini, M., Yu, H., Boschin, F., Magnone, L., Rossini, M., Di Domenico, G., Baruffaldi, F., Oxilia, G., Bortolini, E., Dellù, E., Moroni, A., Ronchitelli, A., Talamo, S., Müller, W., Calattini, M., Nava, A., Posth, C., Lari, M., Bondioli, L., Benazzi, S., Caramelli, D., 2024. Life history and ancestry of the late Upper Palaeolithic infant from Grotta delle Mura, Italy. Nat. Commun. 15, 8248. https://doi.org/10.1038/s41467-024-51150-x.

Hillson, S., 2005. Teeth, second ed. Cambridge University Press. https://doi.org/10.1017/CBO9780511614477.

Hillson, S., 1996. Dental Anthropology, third ed. Cambridge University Press, Cambridge.

Hodgkins, J., Orr, C.M., Gravel-Miguel, C., Riel-Salvatore, J., Miller, C.E., Bondioli, L., Nava, A., Lugli, F., Talamo, S., Hajdinjak, M., Cristiani, E., Romandini, M., Meyer, D., Drohobytsky, D., Kuester, F., Pothier-Bouchard, G., Buckley, M., Mancini, L., Baruffaldi, F., Silvestrini, S., Arrighi, S., Keller, H.M., Griggs, R.B., Peresani, M., Strait, D.S., Benazzi, S., Negrino, F., 2021. An infant burial from Arma Veirana in northwestern Italy provides insights into funerary practices and female personhood in early Mesolithic Europe. Sci. Rep. 8. https://doi.org/10.1038/s41598-021-02804-z.

Hosek, L., Robb, J., 2019. Osteobiography: a platform for bioarchaeological research. Bioarchaeol Int 3, 1–15. https://doi.org/10.5744/BI.2019.1005.

Kamenov, G.D., Lofaro, E.M., Goad, G., Krigbaum, J., 2018. Trace elements in modern and archaeological human teeth: implications for human metal exposure and enamel diagenetic changes. J. Archaeol. Sci. 99, 27–34. https://doi.org/10.1016/j.jas.2018.09.002.

Kapp, J.D., Green, R.E., Shapiro, B., 2021. A fast and efficient single-stranded genomic Library preparation method optimized for Ancient DNA. J. Hered. 112, 241–249. https://doi.org/10.1093/jhered/esab012.

Longin, R., 1971. No title. Nature 230, 241–242. https://doi.org/10.1038/230241a0.

Lugli, F., Cipriani, A., Capecchi, G., Ricci, S., Boschin, F., Boscato, P., Iacumin, P., Badino, F., Mannino, M.A., Talamo, S., Richards, M.P., Benazzi, S., Ronchitelli, A., 2019a. Strontium and stable isotope evidence of human mobility strategies across the Last Glacial Maximum in southern Italy. Nat Ecol Evol 3, 905–911. https://doi.org/10.1038/s41559-019-0900-8.

Lugli, F., Di Rocco, G., Vazzana, A., Genovese, F., Pinetti, D., Cilli, E., Carile, M.C., Silvestrini, S., Gabanini, G., Arrighi, S., Buti, L., Bortolini, E., Cipriani, A., Figus, C., Marciani, G., Oxilia, G., Romandini, M., Sorrentino, R., Sola, M., Benazzi, S., 2019b. Enamel peptides reveal the sex of the Late Antique 'Lovers of Modena. Sci. Rep. 9, 1–8. https://doi.org/10.1038/s41598-019-49562-7.

Lugli, F., Figus, C., Silvestrini, S., Costa, V., Bortolini, E., Conti, S., Peripoli, B., Nava, A., Sperduti, A., Lamanna, L., Bondioli, L., Benazzi, S., 2020. Sex-related morbidity and mortality in non-adult individuals from the Early Medieval site of Valdaro (Italy): the contribution of dental enamel peptide analysis. J Archaeol Sci Rep 34, 102625. https://doi.org/10.1016/j.jasrep.2020.102625.

Lugli, F., Nava, A., Sorrentino, R., Vazzana, A., Bortolini, E., Oxilia, G., Silvestrini, S., Nannini, N., Bondioli, L., Fewlass, H., Talamo, S., Bard, E., Mancini, L., Müller, W., Romandini, M., Benazzi, S., 2022. Tracing the mobility of a Late Epigravettian (~ 13 ka) male infant from Grotte di Pradis (Northeastern Italian Prealps) at high-temporal resolution. Sci. Rep. https://doi.org/10.1038/s41598-022-12193-6.

Magri, S., Higgins, O.A., Lugli, F., Silvestrini, S., Vazzana, A., Bondioli, L., Nava, A., Benazzi, S., 2024. Enamel Histomorphometry, Growth Patterns and Developmental Trajectories of the First Deciduous Molar in an Italian Early Medieval Skeletal Series. bioRxiv. https://doi.org/10.1101/2024.05.13.593149.

Mahoney, P., 2015. Dental fast track: prenatal enamel growth, incisor eruption, and weaning in human infants. Am. J. Phys. Anthropol. 156, 407–421. https://doi.org/10.1002/ajpa.22666.

Mahoney, P., 2012. Incremental enamel development in modern human deciduous anterior teeth. Am. J. Phys. Anthropol. 147, 637–651. https://doi.org/10.1002/ajpa.22029.

Mahoney, P., 2011. Human deciduous mandibular molar incremental enamel development. Am. J. Phys. Anthropol. 144, 204–214. https://doi.org/10.1002/ajpa.21386.
Mahoney, P., 2008. Intraspecific variation in M1 enamel development in modern humans: implications for human evolution. J. Hum. Evol. 55, 131–147. https://doi.org/10.1016/j.jhevol.2008.02.004.
Manifold, B.M., 2012. Intrinsic and extrinsic factors involved in the preservation of non-adult skeletal remains in archaeology and forensic science. Bull. Int. Assoc. Paleodontol. 6 (2), 51–69.
Maricic, T., Whitten, M., Pääbo, S., 2010. Multiplexed DNA sequence capture of mitochondrial genomes using PCR products. PLoS One 5, e14004. https://doi.org/10.1371/journal.pone.0014004.
McFarlane, G., Loch, C., Guatelli-Steinberg, D., Bayle, P., Le Luyer, M., Sabel, N., Nava, A., Floyd, B., Skinner, M., White, S., Pitfield, R., Mahoney, P., 2021. Enamel daily secretion rates of deciduous molars from a global sample of children. Arch. Oral Biol. 132. https://doi.org/10.1016/j.archoralbio.2021.105290.
Miari, M., Bestetti, F., Rasia, P.A., 2017. La Necropoli Eneolitica Di Celletta Dei Passeri (Forlì): Analisi Delle Sepolture E Dei Corredi Funerari, LXVII. Rivista di Scienze Preistoriche, pp. 145–208. https://doi.org/10.32097/1005.
Mittnik, A., Wang, C.-C., Svoboda, J., Krause, J., 2016. A molecular approach to the sexing of the triple burial at the upper Paleolithic site of dolní věstonice. PLoS One 11, e0163019. https://doi.org/10.1371/journal.pone.0163019.
Moorrees, C.F.A., Fanning, E.A., Hunt, E.E., 1963a. Formation and resorption of three deciduous teeth in children. Am. J. Phys. Anthropol. 21, 205–213. https://doi.org/10.1002/AJPA.1330210212.
Moorrees, C.F.A., Fanning, E.A., Hunt, E.E., 1963b. Age variation of formation stages for ten permanent teeth. J. Dent. Res. 42, 1490–1502. https://doi.org/10.1177/00220345630420062701.
Morico, G., 1997. Il pozzo della Panighina. In: Pacciarelli, M. (Ed.), Acque, Grotte E Dei: 3000 Anni Di Culti Preromani in Romagna, Marche E Abruzzo. Morandi, Imola.
Morico, G., 1996. Pagihina di Bertinoro, Forli. In: Bermond Montanari, G., Massi Pasi, M., Prati, L. (Eds.), Quando Forli Non C'Era: Origine Del Territorio E Popolamento Umano Dal Paleolitico Al IV Sec. A.C. Abaco Edizioni, Forlì.
Müller, W., Lugli, F., McCormack, J., Evans, D., Anczkiewicz, R., Bondioli, L., Nava, A., 2024. Human life histories. In: Anbar, A., Weis, D. (Eds.), Treatise on Geochemistry. Elsevier, Oxford, pp. 281–328.
Müller, W., Nava, A., Evans, D., Rossi, P.F., Alt, K.W., Bondioli, L., 2019a. Enamel mineralization and compositional time-resolution in human teeth evaluated via histologically-defined LA-ICPMS profiles. Geochem. Cosmochim. Acta 255, 105–126. https://doi.org/10.1016/j.gca.2019.03.005.
Müller, W., Nava, A., Evans, D., Rossi, P.F., Alt, K.W., Bondioli, L., 2019b. Enamel mineralization and compositional time-resolution in human teeth evaluated via histologically-defined LA-ICPMS profiles. Geochem. Cosmochim. Acta 255, 105–126. https://doi.org/10.1016/j.gca.2019.03.005.
Nava, A., Bondioli, L., Coppa, A., Dean, C., Rossi, P.F., Zanolli, C., 2017a. New regression formula to estimate the prenatal crown formation time of human deciduous central incisors derived from a Roman Imperial sample (Velia, Salerno, Italy, I-II cent. CE). PLoS One 12, e0180104. https://doi.org/10.1371/journal.pone.0180104.
Nava, A., Coppa, A., Coppola, D., Mancini, L., Dreossi, Di, Zanini, F., Bernardini, F., Tuniz, C., Bondioli, L., 2017b. Virtual histological assessment of the prenatal life history and age at death of the Upper Paleolithic fetus from Ostuni (Italy). Sci. Rep. 7, 1–10. https://doi.org/10.1038/s41598-017-09773-2.
Nava, A., Frayer, D.W., Bondioli, L., 2019. Longitudinal analysis of the microscopic dental enamel defects of children in the Imperial Roman community of Portus Romae (Necropolis of Isola Sacra, 2nd to 4th century CE, Italy). J Archaeol Sci Rep 23, 406–415. https://doi.org/10.1016/J.JASREP.2018.11.007.
Nava, A., Lugli, F., Lemmers, S., Cerrito, P., Mahoney, P., Bondioli, L., Müller, W., 2024. Reading children's teeth to reconstruct life history and the evolution of human cooperation and cognition: the role of dental enamel microstructure and chemistry. Neurosci. Biobehav. Rev. 163, 105745. https://doi.org/10.1016/j.neubiorev.2024.105745.
Nava, A., Lugli, F., Romandini, M., Badino, F., Evans, D., Helbling, A.H., Oxilia, G., Arrighi, S., Bortolini, E., Delpiano, D., Duches, R., Figus, C., Livraghi, A., Marciani, G., Silvestrini, S., Cipriani, A., Giovanardi, T., Pini, R., Tuniz, C., Bernardini, F., Dori, I., Coppa, A., Cristiani, E., Dean, C., Bondioli, L., Peresani, M., Müller, W., Benazzi, S., 2020. Early life of neanderthals. Proc. Natl. Acad. Sci. U. S. A. 117, 28719–28726. https://doi.org/10.1073/pnas.2011765117.
Neukamm, J., Peltzer, A., Nieselt, K., 2021. DamageProfiler: fast damage pattern calculation for ancient DNA. Bioinformatics 37, 3652–3653. https://doi.org/10.1093/bioinformatics/btab190.
Olalde, I., Brace, S., Allentoft, M.E., Armit, I., Kristiansen, K., Booth, T., Rohland, N., Mallick, S., Szécsényi-Nagy, A., Mittnik, A., Altena, E., Lipson, M., Lazaridis, I., Harper, T.K., Patterson, N., Broomandkhoshbacht, N., Diekmann, Y., Faltyskova, Z., Fernandes, D., Ferry, M., Harney, E., De Knijff, P., Michel, M., Oppenheimer, J., Stewardson, K., Barclay, A., Alt, K.W., Liesau, C., Rios, P., Blasco, C., Miguel, J.V., Garcia, R.M., Fernandez, A.A., Banffy, E., Bernabo-Brea, M., Billoin, D., Bonsall, C., Bonsall, L., Allen, T., Buster, L., Carver, S., Navarro, L.C., Craig, O.E., Cook, G.T., Cunliffe, B., Denaire, A., Dinwiddy, K.E., Dodwell, N., Ernee, M., Evans, C., Kucharik, M., Farre, J.F., Fowler, C., Gazenbeek, M., Pena, R.G., Haber-Uriarte, M., Haduch, E., Hey, G., Jowett, N., Knowles, T., Massy, K., Pfrengle, S., Lefranc, P., Lemercier, O., Lefebvre, A., Martinez, C.H., Olmo, V.G., Ramirez, A.B., Maurandi, J. L., Majo, T., McKinley, J.I., McSweeney, K., Mende, B.G., Mod, A., Kulcsar, G., Kiss, V., Czene, A., Patay, R., Endrodi, A., Kohler, K., Hajdu, T., Szeniczey, T., Dani, J., Bernert, Z., Hoole, M., Cheronet, O., Keating, D., Veleminsky, P., Dobe, M., Candilio, F., Brown, F., Fernandez, R.F., Herrero-Corral, A.M., Tusa, S., Carnieri, E., Lentini, L., Valenti, A., Zanini, A., Waddington, C., Delibes, G., Guerra-Doce, E., Neil, B., Brittain, M., Luke, M., Mortimer, R., Desideri, J., Besse, M., Brucken, G., Furmanek, M., Hauszko, A., Mackiewicz, M., Rapinski, A., Leach, S., Soriano, I., Lillios, K.T., Cardoso, J.L., Pearson, M.P., Wodarczak, P., Price, T.D., Prieto, P., Rey, P.J., Risch, R., Guerra, M.A.R., Schmitt, A., Serralongue, J., Silva, A.M., Smrcka, V., Vergnaud, L., Zilhao, J., Caramelli, D., Higham, T., Thomas, M.G., Kennett, D.J., Fokkens, H., Heyd, V., Sheridan, A., Sjogren, K.G., Stockhammer, P. W., Krause, J., Pinhasi, R., Haak, W., Barnes, I., Lalueza-Fox, C., Reich, D., 2018. The Beaker phenomenon and the genomic transformation of northwest Europe. Nature 555, 190–196. https://doi.org/10.1038/nature25738.
Olalde, I., Mallick, S., Patterson, N., Rohland, N., Villalba-Mouco, V., Silva, M., Dulias, K., Edwards, C.J., Gandini, F., Pala, M., Soares, P., Ferrando-Bernal, M., Adamski, N., Broomandkhoshbacht, N., Cheronet, O., Culleton, B.J., Fernandes, D., Lawson, A.M., Mah, M., Oppenheimer, J., Stewardson, K., Zhang, Z., Arenas, J.M.J., Moyano, I.J.T., Salazar-García, D.C., Castanyer, P., Santos, M., Tremoleda, J., Lozano, M., Borja, P.G., Fernández-Eraso, J., Mujika-Alustiza, J.A., Barroso, C., Bermúdez, F.J., Mínguez, E.V., Burch, J., Coromina, N., Vivó, D., Cebrià, A., Fullola, J.M., García-Puchol, O., Morales, J.I., Xavier Oms, F., Majó, T., Vergès, J.M., Díaz-Carvajal, A., Ollich-Castanyer, I., Javier López-Cachero, F., Silva, A.M., Alonso-Fernández, C., De Castro, G.D., Echevarría, J.J., Moreno-Márquez, A., Berlanga, G.P., Ramos-García, P., Ramos-Muñoz, J., Vila, E.V., Arzo, G.A., Arroyo, Á.E., Lillios, K.T., Mack, J., Velasco-Vázquez, J., Waterman, A., De Lugo Enrich, L.B., Sánchez, M.B., Agustí, B., Codina, F., De Prado, G., Estalrrich, A., Flores, Á.F., Finlayson, C., Finlayson, G., Finlayson, S., Giles-Guzmán, F., Rosas, A., González, V.B., Atiénzar, G. G., Hernández Pérez, M.S., Llanos, A., Marco, Y.C., Beneyto, I.C., López-Serrano, D., Tormo, M.S., Valera, A.C., Blasco, C., Liesau, C., Ríos, P., Daura, J., De Pedro Michó, M.J., Diez-Castillo, A.A., Fernández, R.F., Farré, J.F., Garrido-Pena, R., Gonçalves, V.S., Guerra-Doce, E., Herrero-Corral, A.M., Juan-Cabanilles, J., López-Reyes, D., McClure, S.B., Pérez, M.M., Foix, A.O., Borràs, M.S., Sousa, A.C., Encinas, J.M.V., Kennett, D.J., Richards, M.B., Alt, K.W., Haak, W., Pinhasi, R., Lalueza-Fox, C., Reich, D., 2019. The genomic history of the Iberian Peninsula over the past 8000 years. Science 363, 1230–1234. https://doi.org/10.1126/science.aav4040, 1979.
Parker, C., Rohrlach, A.B., Friederich, S., Nagel, S., Meyer, M., Krause, J., Bos, K.I., Haak, W., 2020. A systematic investigation of human DNA preservation in medieval skeletons. Sci. Rep. 10, 1–16. https://doi.org/10.1038/s41598-020-75163-w.
Pinhasi, R., Fernandes, D., Sirak, K., Novak, M., Connell, S., Alpaslan-Roodenberg, S., Gerritsen, F., Moiseyev, V., Gromov, A., Raczky, P., Anders, A., Pietrusewsky, M., Rollefson, G., Jovanovic, M., Trinhhoang, H., Bar-Oz, G., Oxenham, M., Matsumura, H., Hofreiter, M., 2015. Optimal ancient DNA yields from the inner ear part of the human petrous bone. PLoS One 10. https://doi.org/10.1371/journal.pone.0129102.
R Core Team, 2023. R: a Language and Environment for Statistical Computing. R Foundation for Statistical Computing.
Reid, D.J., Beynon, A.D., Ramirez Rozzi, F.V., 1998. Histological reconstruction of dental development in four individuals from a medieval site in Picardie, France. J. Hum. Evol. 35, 463–477. https://doi.org/10.1006/jhev.1998.0233.
Reid, D.J., Dean, M.C., 2006. Variation in modern human enamel formation times. J. Hum. Evol. 50, 329–346. https://doi.org/10.1016/J.JHEVOL.2005.09.003.
Renaud, G., Slon, V., Duggan, A.T., Kelso, J., 2015. Schmutzi: estimation of contamination and endogenous mitochondrial consensus calling for ancient DNA. Genome Biol. 16, 224. https://doi.org/10.1186/s13059-015-0776-0.
Reynard, B., Balter, V., 2014. Trace elements and their isotopes in bones and teeth: Diet, environments, diagenesis, and dating of archeological and paleontological samples. Palaeogeogr. Palaeoclimatol. Palaeoecol. 416, 4–16. https://doi.org/10.1016/J.PALAEO.2014.07.038.
Robinson, J.T., Thorvaldsdóttir, H., Winckler, W., Guttman, M., Lander, E.S., Getz, G., Mesirov, J.P., 2011. Integrative genomics viewer. Nat. Biotechnol. https://doi.org/10.1038/nbt.1754.
Sabel, N., Johansson, C., Kühnisch, J., Robertson, A., Steiniger, F., Norén, J.G., Klingberg, G., Nietzsche, S., 2008. Neonatal lines in the enamel of primary teeth—A morphological and scanning electron microscopic investigation. Arch. Oral Biol. 53, 954–963. https://doi.org/10.1016/J.ARCHORALBIO.2008.05.003.
Schindelin, J., Arganda-Carreras, I., Frise, E., Kaynig, V., Longair, M., Pietzsch, T., Preibisch, S., Rueden, C., Saalfeld, S., Schmid, B., Tinevez, J.Y., White, D.J., Hartenstein, V., Eliceiri, K., Tomancak, P., Cardona, A., 2012. Fiji: an open-source platform for biological-image analysis. Nat. Methods. https://doi.org/10.1038/nmeth.2019.
Secher, B., Fregel, R., Larruga, J.M., Cabrera, V.M., Endicott, P., Pestano, J.J., González, A.M., 2014. The history of the North African mitochondrial DNA haplogroup U6 gene flow into the African, Eurasian and American continents. BMC Evol. Biol. 14, 109. https://doi.org/10.1186/1471-2148-14-109.
Shepherd, T.J., Dirks, W., Manmee, C., Hodgson, S., Banks, D.A., Averley, P., Pless-Mulloli, T., 2012. Reconstructing the life-time lead exposure in children using dentine in deciduous teeth. Sci. Total Environ. 425, 214–222. https://doi.org/10.1016/j.scitotenv.2012.03.022.
Sirak, K., Fernandes, D., Cheronet, O., Harney, E., Mah, M., Mallick, S., Rohland, N., Adamski, N., Broomandkhoshbacht, N., Callan, K., Candilio, F., Lawson, A.M., Mandl, K., Oppenheimer, J., Stewardson, K., Zalzala, F., Anders, A., Bartík, J., Coppa, A., Dashtseveg, T., Évinger, S., Farkaš, Z., Hajdu, T., Bayarsaikhan, J., McIntyre, L., Moiseyev, V., Okumura, M., Pap, I., Pietrusewsky, M., Raczky, P., Šefčáková, A., Soficaru, A., Szeniczey, T., Szoke, B.M., van Gerven, D., Vasilyev, S., Bell, L., Reich, D., Pinhasi, R., 2020. Human auditory ossicles as an alternative optimal source of ancient DNA. Genome Res. 30, 427–436. https://doi.org/10.1101/gr.260141.119.
Smith, T.M., Austin, C., Green, D.R., Joannes-Boyau, R., Bailey, S., Dumitriu, D., Fallon, S., Grün, R., James, H.F., Moncel, M.H., Williams, I.S., Wood, R., Arora, M.,

2018. Wintertime stress, nursing, and lead exposure in Neanderthal children. Sci. Adv. 4, eaau9483. https://doi.org/10.1126/sciadv.aau9483.
Smith, T.M., Reid, D.J., Olejniczak, A.J., Bailey, S., Glantz, M., Viola, B., Hublin, J.J., 2011. Dental development and age at death of a middle paleolithic juvenile hominin from Obi-Rakhmat Grotto, Uzbekistan. In: Vertebrate Paleobiology and Paleoanthropology. Springer, pp. 155–163. https://doi.org/10.1007/978-94-007-0492-3_13.
Smith, T.M., Tafforeau, P., Reid, D.J., Pouech, J., Lazzari, V., Zermeno, J.P., Guatelli-Steinberg, D., Olejniczak, A.J., Hoffman, A., Radovčić, J., Makaremi, M., Toussaint, M., Stringer, C., Hublin, J.J., 2010. Dental evidence for ontogenetic differences between modern humans and Neanderthals. Proc. Natl. Acad. Sci. U. S. A. 107, 20923–20928. https://doi.org/10.1073/pnas.1010906107.
Stewart, N.A., Gerlach, R.F., Gowland, R.L., Gron, K.J., Montgomery, J., 2017. Sex determination of human remains from peptides in tooth enamel. Proc. Natl. Acad. Sci. U. S. A. 114, 13649–13654. https://doi.org/10.1073/pnas.1714926115.
Tambets, K., Rootsi, S., Kivisild, T., Help, H., Serk, P., Loogväli, E.L., Tolk, H.V., Reidla, M., Metspalu, E., Pliss, L., Balanovsky, O., Pshenichnov, A., Balanovska, E., Gubina, M., Zhadanov, S., Osipova, L., Damba, L., Voevoda, M., Kutuev, I., Bermisheva, M., Khusnutdinova, E., Gusar, V., Grechanina, E., Parik, J., Pennarun, E., Richard, C., Chaventre, A., Moisan, J.P., Barać, L., Peričić, M., Rudan, P., Terzić, R., Mikerezi, I., Krumina, A., Baumanis, V., Koziel, S., Rickards, O., De Stefano, G.F., Anagnou, N., Pappa, K.I., Michalodimitrakis, E., Ferák, V., Füredi, S., Komel, R., Beckman, L., Villems, R., 2004. The Western and eastern roots of the saami - the story of genetic "Outliers" told by mitochondrial DNA and Y chromosomes. Am. J. Hum. Genet. 74, 661–682. https://doi.org/10.1086/383203.
Torroni, A., Bandelt, H.J., D'Urbano, L., Lahermo, P., Moral, P., Sellitto, D., Rengo, C., Forster, P., Savontaus, M.L., Bonné-Tamir, B., Scozzari, R., 1998. mtDNA analysis reveals a major late paleolithic population expansion from southwestern to northeastern Europe. Am. J. Hum. Genet. 62, 1137–1152. https://doi.org/10.1086/301822.
Villalba-Mouco, V., Oliart, C., Rihuete-Herrada, C., Childebayeva, A., Rohrlach, A.B., Fregeiro, M.I., Beltrán, E.C., Velasco-Felipe, C., Aron, F., Himmel, M., Freund, C., Alt, K.W., Salazar-García, D.C., Atiénzar, G.G., De Miguel Ibáñez, M.P., Pérez, M.S. H., Barciela, V., Romero, A., Ponce, J., Martínez, A., Lomba, J., Soler, J., Martínez, A. P., Fernández, A.A., Haber-Uriarte, M., De Togores Muñoz, C.R., Olalde, I., Lalueza-Fox, C., Reich, D., Krause, J., Sanjuán, L.G., Lull, V., Micó, R., Risch, R., Haak, W., 2021. Genomic transformation and social organization during the Copper Age-Bronze Age transition in southern Iberia. Sci. Adv. 7. https://doi.org/10.1126/sciadv.abi7038.
White, T., Folkens, P., 2005. The human bone manual. The Human Bone Manual. Elsevier Inc. https://doi.org/10.1016/C2009-0-00102-0.
Willmes, M., Kinsley, L., Moncel, M.H., Armstrong, R.A., Aubert, M., Eggins, S., Grün, R., 2016. Improvement of laser ablation in situ micro-analysis to identify diagenetic alteration and measure strontium isotope ratios in fossil human teeth. J. Archaeol. Sci. 70, 102–116. https://doi.org/10.1016/J.JAS.2016.04.017.
Wilson, D.F., Shroff, F.R., 1970. The nature of the striæ of Retzius as seen with the optical microscope. Aust. Dent. J. 15, 162–171. https://doi.org/10.1111/j.1834-7819.1970.tb03366.x.
Wilson, L., Pollard, A.M., 2002. Here today, gone tomorrow? Integrated experimentation and geochemical modeling in studies of archaeological diagenetic change. Acc. Chem. Res. 35, 644–651. https://doi.org/10.1021/ar000203s.
Wrobel, G.D., Cucina, A., 2024. Mesoamerican osteobiographies: revealing the lives and deaths of Ancient individuals. Mesoamerican Osteobiographies, first ed. University of Florida Press. https://doi.org/10.2307/JJ.16430753.